Topology switch between AIE and ACQ: a balance of substituents

Patryk Rybczyński,*,[a] Tadeusz M. Muzioł,[a] Anna Kaczmarek-Kędziera,[a] Borys Ośmiałowski*,[a]

Intermolecular interactions appearing in solution, aggregates and solid state are known to affect the photophysical properties of fluorophores, leading either to emission quenching or to emission enhancement upon aggregation. The novel strategy for the aggregation-induced fluorescence change based upon the subtle balance of the intermolecular and intramolecular charge transfer in the benzothiazole derivatives is presented here, leading to the extremely bright aggregates of the compounds dark in solution or vice versa. The introduction of the two different mild substituents into the fluorophore core results in two regioisomers exhibiting the same crystal packing, but extremely different behavior upon aggregation. Such an approach opens a simple way of controlling the AIE/ACQ behavior of small molecules in the wide range of FQY values.

Over the last decades, the number of dyes with appealing photophysical properties has drastically increased, allowing development of novel fluorescence-based technologies such as OLEDs [1–3], sensors [4–6] or bio-labeling [7–9]. Application of fluorescent materials requires a thorough understanding of the behavior of molecules in variable environments with emphasis on controlling photophysical properties in the intramolecular and intermolecular regimes. In that regard, the sensitivity of the dye introduced by the *intra*molecular charge-transfer (ICT) can be monitored by changes in absorption, emission, Stokes shift, and fluorescence quantum yield (FQY). The *inter*molecular forces, such as hydrogen and halogen bonds [10,11] or stacking can lead to aggregation, which affects the same set of photophysical properties, providing the aggregation-induced emission (AIE) or aggregation-caused quenching (ACQ) mechanisms for FQY control. The number of structural features of a molecule (rigidity/flexibility, proton transfer, hydrophobic/hydrophilic nature of dye) deliver the technical tools to influence subtle intermolecular interactions and thus achieve desired aggregation-induced emission change.

The systematic modification of the dye environment, from the solution with dominating dye-solvent interactions, via aggregate, where the influence of solvent molecules is reduced in favour of dye-dye interaction, can be concluded with the crystal structure, appearing as the extreme aggregate case in the absence of solvent molecules. While for most of aromatic, planar and rigid fluorophores, usually fluorescent in solution, the emission in solid deteriorates due to stacking-assisted ACQ [12], the main principle in design of AIE molecules is based on the introduction of solution-flexible molecular structures [13–15], which minimize intramolecular motion [16] when aggregated. This limits the non-radiative transition pathways, shifting towards radiative decay and thus increasing FQY. On the other hand, from the structural point of view, sterically hindered substituents can prevent close packing leading to reduced intermolecular interactions and suppression of ACQ.

The rational selection of a character, size and placement of substituents in the dye is vital for obtaining their desirable properties. [17,18] It has been shown that the orderly change of electron-donating/withdrawing substituents in fluorophores affects non-radiative rate constants in a linear way. [19–21] On the othre hand, it has been demonstrated that the regioisomers of anthracene [22] exhibit the AIE behaviour in two among five investigated derivatives, whereas the triphenylamine-decorated benzo[*i*]dithiophenephenazines can be transformed from the ACQ to AIE form via modification of their crystal packing caused by relocation of electron-donating substituents - increase of FQY by more than 15%. [23]

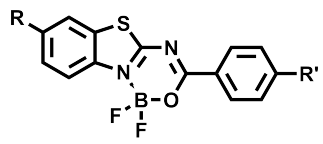

R/R' =

OMe/OMe	(**1**)	H/OMe	(**4**)	CF_3/OMe	(**7**)
OMe/H	(**2**)	H/H	(**5**)	CF_3/H	(**8**)
OMe/CF_3	(**3**)	H/CF_3	(**6**)	CF_3/CF_3	(**9**)

Scheme 1. Structure of investigated compounds

The applications of AIE-dyes in bioimaging exploits their sensitivity to viscosity and the concentration of specific proteins. [24] The classical example, Thioflavin T (ThT), binds to β-amyloid fibrils by interaction of its -NMe_2 group perpendicularly aligned [25,26] to the peptide assembly surface. The drawbacks arising from the weak photophysical response of ThT can be removed by proper substitution of the molecular skeleton, [27] however the cationic nature limiting its efficient aggregation and compatibility to the hydrophobic protein pockets still needs to be worked out. The remedy for this problem is proposed in the present study. The series of the dyes, shown in Scheme 1, possess the two parts of fluorophore still separated by single bond allowing to conformational equlibrium to take place. The previous study devoted to their properties in solution, indicated that the efficient FQY control can be obtained by the proper substitution with even mildly donating (**D**) or accepting (**A**) substituents. It was proven that both the strength of the push-pull effect and its direction affects the emission, and the presence of the two different substituents in the fluorescent core can cover the whole range of the FQY values. [28] Here, the strategy based on the topology switch for the AIE-ACQ

[a] Faculty of Chemistry, Nicolaus Copernicus University in Toruń, Gagarina Street 7, 87-100 Toruń, Poland
E-mail: pat_ryb@doktorant.umk.pl, borys.osmialowski@umk.pl

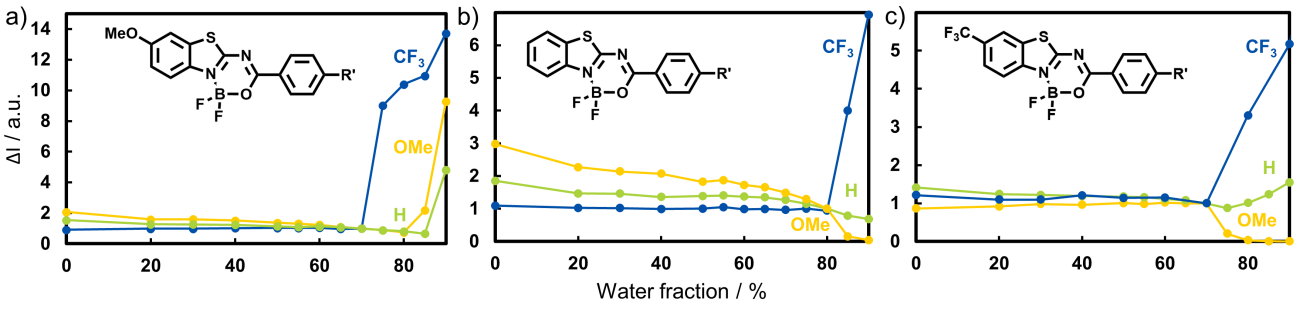

Figure 1. Normalized changes in fluorescence intensity (ΔI) for the investigated systems at maximum emission: (a) **1–3**, (b) **4–6**, (c) **7–9**

control is developed. Fluorescence of nine dyes, including pairs of regioisomers, is compared for solution, aggregates and solid state and discussed with support of theoretical approach, in comparison to previously reported analog bearing strong electron-donor.[29]

Upon aggregation (THF/water), the absorption spectra of **1-9** show a significant decrease in absorbance and alterations in the shape of bands as the aggregation proceeds. In general, the position of absorption does not change much except for dyes with R=CF_3 (hypsochromic shift) and compound **1** (broad and complicated spectrum), while the modulation of emission upon aggregation depends on the substituents.

AIE/ACQ effects are presented in Fig. 1. The emission intensities were normalized to 1 at the point where the AIE starts for dyes with R′=CF_3. The presence of CF_3 group attached to phenyl (dyes **3**, **6** and **9**), regardless of R, introduces AIE behavior with a lower THF/water ratio than for the H– or OMe–substituted phenyls (blue lines, Fig. 1). The highest increase of emission intensity, compared to the dilute THF solution, was observed for compound **3** featuring **DAA** topology (blue, Fig. 1a). On the other hand, the most efficient quenching of emission occurs for compound **7**, isomer of **3**, representing **AAD** pattern (yellow, Fig. 1c). Although the introduction of hydrophobic (CF_3) or slightly hydrophylic (OMe) substituents can be useful from biomedical point of view, the comparison of regioisomers **3** and **7** reveal that substituents' flip controls aggregation-assisted fluorescence change. Similarly, the opposite behavior is observed for **2** and **4**, but not for **6** and **8**, suggesting that for the effective switching between AIE and ACQ the donor group is essential, a structural feature not fulfilled for **6** and **8**.

The number of variables in the analyzed systems, in particular the presence of the two different substituents at various positions, which effect is not simply additive, makes the generalization of observed tendencies not straightforward. Yet, the triplets of the dyes, differing with one substituent only can be directly compared. Hence, for compounds carrying electron OMe group in the benzothiazole ring (**1-3**) fluorescence is enhanced upon aggregation. For compounds within sub-groups **4-6** and **7-9** the AIE is observed for strong electron acceptor at R′, slight increase or decrease of emission (absence of substituent), and finally ACQ in the presence of electron donor OMe attached to phenyl (Fig. 1b and 1c.) The FQY data suggests that for aggregates of sub-group **1-3**, the excited state potential energy surface is high above the ground state and, most probably, the conical intersection is energetically separated from Franck-Condon excited state, thus limiting a non-radiative decay probability and causing emission enhancement (compare[28]). The similar conclusion can be drawn for the remaining -$C_6H_4CF_3$ dyes (**6** and **9**).

Table 1. Maximum of absorption in THF, maximum of emission in THF, THF/water aggregate (97% water) and in the solid state for **1-9**

Comp.	Topology	λ^{abs}_{THF}	λ^{em}_{THF}	λ^{em}_{agg}	λ^{em}_{solid}
1	**DAD**	366.5	457.5	471.5	472.5
2	**DA-**	361.0	464.0	464.5	486.5
3	**DAA**	366.0	496.0	483.5	511.0
4	**-AD**	362.0	419.0	476.5	485.0
5	**-A-**	341.5	445.0	450.5	442.5
6	**-AA**	344.0	451.0	453.5	451.5
7	**AAD**	361.0	413.0	508.0	495.0
8	**AA-**	338.0	428.0	442.5	442.5
9	**AAA**	339.5	451.5	458.0	441.5

The emission wavelength (Tab. 1) for the molecule depends on the nearest surrounding of the dye. In the series **1-3** (R=OMe), upon aggregation the bathochromic shift is visible for the first compound, no change in the emission for **2**, and hypsochromic shift for **3**. Within the sub-series **4-6** (R=H), for compounds **5** and **6** (R′=H and CF_3), the red-shift is very small and amounts to 5.5 and 2.5 nm, respectively. On the other hand, for **7-9** compounds with R′=H or CF_3, the emission red-shift upon aggregation is much smaller than that for **7**, but this is not surprising as **7** is extreme molecule (*vide infra*). Thus, for **4** and **7** (R′=OMe, two ACQ dyes) an exceptional red-shift of emission is observed (57.5 and 95 nm, respectively) for an aggregate (λ^{em}_{agg}) with respect to the THF solution (λ^{em}_{THF}). This may be interpreted, in part, as the result of *energy-gap rule* telling that lowering energy between excited and ground states (corresponding to batochromic shift of emission) causes higher probability of non-radiative transitions (FQY decrease). From the supramolecular point of view the origin of such reduction in FQY may lay in both the dye-dye interactions and interaction of dye aggregates with water molecules, however the comparison of the aggregate with crystal data suggest the domination of the latter effect (Tab. S1).

As reported previously, changing the position of the electron donor in the dye can affect the AIE/ACQ behavior.[22] In the present study such a pair of regioisomers is repre-

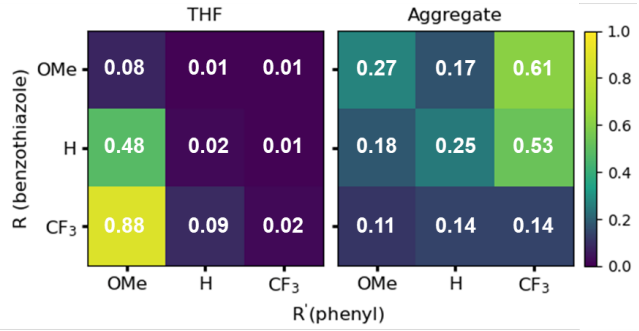

Figure 2. Heatmaps for FQY for **1-9** in THF, suspension in THF/water (97% water) and in the solid state

sented by compounds **2** and **4**. As a result of aggregation, the fluorescence quantum yield for compound **2** increases 17-fold, while for compound **4** the fluorescence quantum yield decreases from 0.48 to 0.18. The introduction of strong electron donor is expected to intensify the described behavior (compare Ref.[22]). Furthermore, introduction of the second substituent of the opposite, electron-accepting, character in the **3** and **7** pair of regioisomers, indicates the opposite molecular topology is the driving force of the opposite mechanisms associated to emission change. The AIE/ACQ effects for such a pair bearing both **D** and **A** substituents is significantly enhanced with respect to only-**D** substituted dyes.

Compound **3** has low FQY (0.01) in THF due to high change of dipole moment upon excitation.[28] In aggregates, the FQY for **3** increases significantly to 0.61, while for **7** decreases from 0.88 (THF) to 0.11. This suggests that AIE arising from the loss of molecular flexibility in **3** is dominant over intermolecular interactions, while ACQ observed in **7** originates from the intermolecular interactions (between dyes and in dye-water regime) in the excited state. Moreover, the crystal structure for these two molecules is very similar (see SI) suggesting similar inter-dye interaction and further supporting water influence on FQY. It is worth mentioning that the difference between energy of emission for **7** in aggregate and in THF solution is equal to 4528 cm^{-1}, a value comparable to the FWHM in THF across the whole series (3536 to 5910 cm^{-1}) and higher than any FWHM for aggregate or solid. This makes **7** the most sensitive dye for its surrounding in the light of its FQY and λ^{em}.

The fluorescence lifetime (Tab. S2) within the series is elongated upon aggregation by 5.5 to 67.9 times and k_r and k_{nr} decrease by 0.6-58.2 times and 1.0-97.9 times, respectively, in all systems but **3** and **6** for radiative and **7** for non-radiative rate constant value.

When one searches the whole dataset for extremes, the molecule **7** is characterised by: *a*) maximum fluorescence lifetime in THF and aggregate, *b*) minimum k_{nr} in THF and aggregate, *c*) minimum k_r in aggregate, but also *d*) maximum k_r in THF. On the contrary, its regioisomer, **3** is characterised by maximum k_r in aggregate and minimal k_r for THF. This means that for AIE-exhibiting fluorophores, the fast non-radiative process, that is promoted in solution, becomes confined in solid due to *restriction of intramolecular rotation or vibration* effect.

The solid-state emission allows to divide the whole series into two groups (Fig. S11): acceptor-only-carrying compounds **5**, **6**, **8** and **9**, with emission maximum around 440 nm and acceptor-donor substituted ones with emission at *ca.* 490 nm (Tab. S1). It is worth to underline the difference in shape and FWHM values for the series (Fig. 3 and S1). It is clear that the spectra for **6** are practically the same in all the environments, while its FQY increases from THF through aggregate to solid. Taking into account **3** and **7** (Fig. 3), their spectra differ to a large extent. For **3**, the emission in all surroundings is very similar to one another, putting aside the vibronic progression, while for its isomeric **7** the aggregate/solid spectrum differs much from THF solution. Thus, **7** can be compared with its counterparts of same topology, described by Potopnyk[29,30], in which electron acceptors (R=CF_3[29]/R=$CF_3C_6H_4$[30]) and strong donor (R′=NMe_2) are attached to the fluorophore skeleton. Both **7** and its NMe_2-substituted counterpart[29,30] crystallize in P-1 triclinic space group and exhibit similar head-to-tail crystal packing, retaining planar structure with the phenyl torsion angle below 1° and similar dye-dye interaction pattern. However, in contrast to **7**, R′=NMe_2-derivative undergoes strong ACQ, decreasing the FQY from 0.61 in THF solution to less than 0.06 in solid state. Since crystal packing in both systems is to the high extend similar, the quenching arises rather from the presence of strong electron-donating dimethylamino group, which develops stronger intramolecular charge transfer than the one due to the milder donating OMe group in **7**.

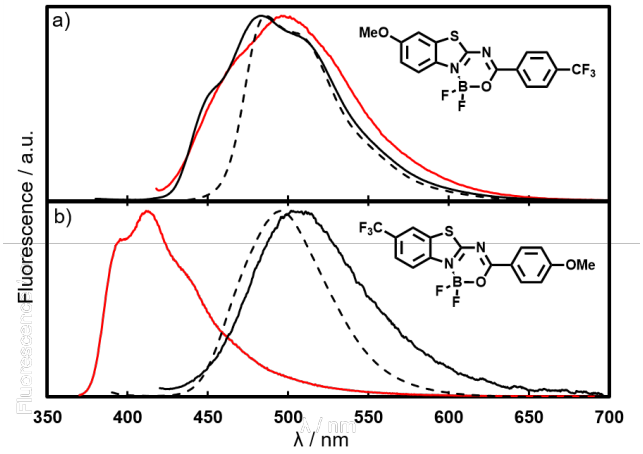

Figure 3. Fluorescence spectra for compounds in solution (red) aggregates (black line) and solid state (dashed line) for (a) **3** and (b) **7**

The ground state intermolecular interaction estimated for the most stable dimers extracted from the crystal (Fig. 4 and S19) confirms the similar nature of interactions in all the systems and the analog from[29]. All the dimers are dispersion-governed, with the dispersion-to-electrostatic ratio significantly exceeding 2.0 (Fig. S8). This unequivocally proves that the factor determining the ACQ/AIE switching is not the stacking interaction in aggregates itself. The Fig. 4 show that energy constituents in **3** and **7** differ from Potopnyk's [**P**].

In summary, the new strategy for the AIE/ACQ control is devised in the present study, exploiting the subtle balance between two different electron-donating/electron-accepting substituents. The modification of the topology of the fluorophore carrying methoxy group provides the effective switching of the emission in the wide range of FQY values yielding bright fluorescence in aggregates and/or solid-

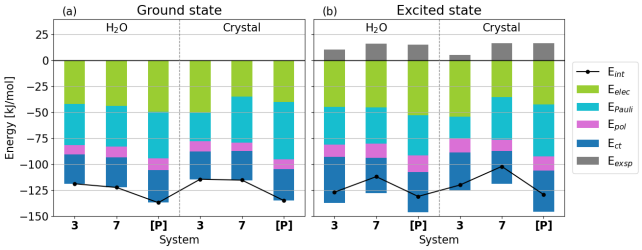

Figure 4. Interaction energy decomposition in ground and excited state for the most stable dimers in water (mimicking the aggregate) and in crystal estimated with ALMO-EDA approach within ωB97X-D/aug-cc-pVDZ for regioisomers **3** and **7** and the dimethylamino derivative[29] (black points denote the total interaction energy, green bars correspond to the electrostatic component, cyan ones – to Pauli term containing exchange and dispersion part, magenta – polarization energy, dark blue – charge transfer contribution and grey in excited state is the excitonic splitting effect)

state. In addition to the previously proposed approaches relying on doubly substituted regioisomers with one type of substituent for crystal packing alterations and substitution by bulky groups for the minimization of internal motion restrictions, current approach opens the plethora of possibilities of simple topology modifications for new effective photoresponsive molecules.

Acknowledgements

Wroclaw Centre for Networking and Supercomputing is gratefully acknowledged for the generous allotment of computational resources. We are very indebted for the Financial support of research from the National Science Centre (project no. 2021/43/B/ST5/00753).

Conflict of Interest

No conflict of interest to declare.

Keywords: aggregation-induced emission • aggregation-caused quenching • emission • fluorescence quantum yield • substituent effect

References

[1] J. Wang, J. Zhang, C. Jiang, C. Yao, X. Xi, *ACS Appl. Mater. Inter.* **2021**, *13*, 57713.
[2] H. Chen, H. Liu, Y. Xiong, J. He, Z. Zhao, B. Z. Tang, *Mater. Chem. Front.* **2022**, *6*, 924.
[3] J. Wang, Y. Yang, C. Jiang, M. He, C. Yao, J. Zhang, *J. Mater. Chem. C* **2022**, *10*, 3163.
[4] D. Wang, B. Z. Tang, *Accounts Chem. Res.* **2019**, *52*, 2559.
[5] M. H. Chua, H. Zhou, Q. Zhu, B. Z. Tang, J. W. Xu, *Mater. Chem. Front.* **2021**, *5*, 659.
[6] M. Gao, B. Z. Tang, *ACS Sensors* **2017**, *2*, 1382.
[7] Y. Wang, J. Nie, W. Fang, L. Yang, Q. Hu, Z. Wang, J. Z. Sun, B. Z. Tang, *Chem. Rev.* **2020**, *120*, 4534.
[8] X. Cai, B. Liu, *Angew. Chem. Int. Edit.* **2020**, *59*, 9868.
[9] T. Zhang, X. Chen, C. Yuan, X. Pang, P. Shangguan, Y. Liu, L. Han, J. Sun, J. W. Y. Lam, Y. Liu, J. Wang, B. Shi, B. Zhong Tang, *Angew. Chem. Int. Ed.* **2023**, *62*, e202211550.
[10] K. Ostrowska, K. M. Stadnicka, M. Gryl, O. Klimas, M. Z. Brela, P. Goszczycki, M. Liberka, J. Grolik, A. Węgrzyn, *Cryst. Growth Des.* **2022**, *22*, 1571.
[11] S. Xie, S. Manuguri, O. Ramström, M. Yan, *Chem.-Asian J.* **2019**, *14*, 910.
[12] C. Xu, T. Wu, L. Duan, Y. Zhou, *Chem. Commun.* **2021**, *57*, 11366.
[13] J. Mei, Y. Hong, J. W. Y. Lam, A. Qin, Y. Tang, B. Z. Tang, *Adv. Mater.* **2014**, *26*, 5429.
[14] Z. He, C. Ke, B. Z. Tang, *ACS Omega* **2018**, *3*, 3267.
[15] T. Wu, J. Huang, Y. Yan, *Chem.–Asian J.* **2019**, *14*, 730.
[16] M. Chen, L. Li, H. Nie, J. Tong, L. Yan, B. Xu, J. Z. Sun, W. Tian, Z. Zhao, A. Qin, B. Z. Tang, *Chem. Sci.* **2015**, *6*, 1932.
[17] P. Meti, H.-S. Lee, Y.-D. Gong, *Dyes Pigments* **2022**, *204*, 110402.
[18] W. Liu, Z. Wang, R. Li, L. Chen, X. Lin, S. Sun, Z. Li, J. Hao, B. Lin, X. Wang, L. Xie, *J. Mol. Struct.* **2022**, *1260*, 132728.
[19] A. Zakrzewska, R. Zaleśny, E. Kolehmainen, B. Ośmiałowski, B. Jędrzejewska, H. Ågren, M. Pietrzak, *Dyes Pigments* **2013**, *99*, 957.
[20] A. M. Grabarz, B. Jędrzejewska, A. Zakrzewska, R. Zaleśny, A. D. Laurent, D. Jacquemin, B. Ośmiałowski, *J. Org. Chem.* **2017**, *82*, 1529.
[21] B. Ośmiałowski, A. Zakrzewska, B. Jędrzejewska, A. Grabarz, R. Zaleśny, W. Bartkowiak, E. Kolehmainen, *J. Org. Chem.* **2015**, *80*, 2072.
[22] S. Sasaki, K. Igawa, G.-i. Konishi, *J. Mater. Chem. C* **2015**, *3*, 5940.
[23] Y. Li, S. Liu, H. Ni, H. Zhang, H. Zhang, C. Chuah, C. Ma, K. S. Wong, J. W. Y. Lam, R. T. K. Kwok, J. Qian, X. Lu, B. Z. Tang, *Angew. Chem. Int. Ed.* **2020**, *59*, 12822.
[24] C. Xue, T. Y. Lin, D. Chang, Z. Guo, *Royal Society Open Science* **2017**, *4*, 160696.
[25] K. J. Robbins, G. Liu, G. Lin, N. D. Lazo, *J. Phys. Chem. Lett* **2011**, *2*, 735.
[26] V. I. Stsiapura, A. A. Maskevich, V. A. Kuzmitsky, V. N. Uversky, I. M. Kuznetsova, K. K. Turoverov, *J. Phys. Chem. B* **2008**, *112*, 15893.
[27] L.-M. Needham, J. Weber, J. A. Varela, J. W. B. Fyfe, D. T. Do, C. K. Xu, L. Tutton, R. Cliffe, B. Keenlyside, D. Klenerman, C. M. Dobson, C. A. Hunter, K. H. Müller, K. O'Holleran, S. E. Bohndiek, T. N. Snaddon, S. F. Lee, *Chem. Sci.* **2020**, *11*, 4578.
[28] P. Rybczyński, M. H. E. Bousquet, A. Kaczmarek-Kędziera, B. Jędrzejewska, D. Jacquemin, B. Ośmiałowski, *Chem. Sci.* **2022**, *13*, 13347.
[29] M. A. Potopnyk, D. Volyniuk, M. Ceborska, P. Cmoch, I. Hladka, Y. Danyliv, J. V. Gražulevičius, *J. Org. Chem.* **2018**, *83*, 12129.
[30] M. A. Potopnyk, D. Volyniuk, R. Luboradzki, M. Ceborska, I. Hladka, Y. Danyliv, J. V. Gražulevičius, *J. Org. Chem.* **2019**, *84*, 5614.